Velocity Spectra of Vortices Scanned with a Pulse-Doppler Radar

DUSAN S. ZRNIC AND RICHARD J. DOVIAK

National Severe Storms Laboratory, NOAA, Norman, Okla. 73069

(Manuscript received 13 February 1975)

ABSTRACT

Doppler velocity spectra of a combined Rankine model vortex are computed by assuming a Gaussian antenna pattern, various vortex sizes, pulse volume depths, and reflectivity profiles. Both very narrow and very broad antenna beamwidths may produce bimodal spectra. Most often, the theoretically derived spectra exhibit a rapid power decrease for spectral components near maximum velocity which agrees with an experimental observation previously reported.

In spring 1973, NSSL's 10 cm, high-resolution Doppler radar scanned the vicinity of a large tornado that devastated Union City, Okla. Digital radar samples were recorded and Fourier-analyzed to derive power spectra for sample volumes spaced about the vortex location. Power spectra were examined for white noise type signatures that indicated vortex rotation contained within the radar sample volume. Spectra were simulated using radar and tornado cyclone parameters matched to those existing during the observations to determine spectral features for comparison with those recorded by the pulse-Doppler radar. The reflectivity throughout and around the funnel was uniform and spectra compared well. Although the precise vortex center location could not be deduced its position was consistent with tornado position determined from film documentation. In the gates containing vortex signatures spectral standard deviations were consistently maximal.

1. Introduction

Two main problems in tornado related studies at present are 1) the detection of tornadoes and 2) velocity measurements within the tornado. While detecting tornadoes is important for the safety of affected population, velocity measurements, in addition to providing data for theoretical modeling studies, also have a very practical use. For example, structures, especially nuclear power plants in tornado prone areas, must be made to resist the maximal tornadic winds. Pulse-Doppler radar offers an optimistic prospect toward the solution to both problems.

So far the most useful maximum velocity measurements were made from tornadic moving pictures (Hoecker, 1960). Those closest to consistently detecting tornadoes through resolution and tracing of mesocyclones are a group from the National Severe Storms Laboratory (Doviak *et al.*, 1974).

It is expected that a very broad and flat Doppler spectrum (white noise type) will be caused by a tornado within the radar pulse volume. Of course, in order to unambiguously resolve all the velocities, the pulse repetition rate must be very high which in turn creates intolerable range ambiguities. In most pulse-Doppler weather radars a compromise between the two ambiguities is made. When the range extent of storm is larger than the unambiguous range interval, folding in range will limit the radars usefulness. Velocity folding is less detrimental to the system since often it can be resolved by judiciously using the fact that mean velocity estimates exhibit a discontinuity when the mean passes through the Nyquist limit, whereas true mean is continuous in range and azimuth.

Until now no numerical Doppler spectrum simulation of a tornado contained in a pulse volume has been made. Lhermitte (1964) calculated the spectrum for a vortex contained entirely within a pulse volume with the vortex model an infinitesimally thin rotating cylinder. Sloss and Atlas (1968) derived an equation for computing spectra from deterministic isodop fields. However, their equation still had an important gradient term missing. Sychra (1972) rigorously derived the essential equations and computed spectral moments by using a simplified one-dimensional tornado model, but he has not computed the resulting spectra. Theoretical spectra, generated by rotating solid and hollow cylinders with uniform antenna gain, were presented by Easterbrook and Joss (1973). In this article we compute Doppler spectra generated by a combined Rankine vortex model having uniform and hollow reflectivity profiles. The antenna pattern is assumed Gaussian and the pulse volume position with respect to the tornado axis is variable. Computed spectra are compared qualitatively with those observed for the first time by a pulse-Doppler radar scanning tornado circulations. This tornado was very large (200–600 m visible diameter) and the region surrounding it had high reflectivity. Furthermore, it's location and path

were determined precisely by a group of laboratory scientists filming its evolution.

2. Simulation of spectra

In this section vortex spectra are simulated for various beamwidths and reflectivity profiles. Vortices are assumed to possess a deterministic radial isodop field. (Randomness of spectral intensity estimates due to reshuffling of scatterers is ignored.) When this field and the reflectivity field are two-dimensional in the x,y plane and the antenna beam axis lies in this plane, the spectra may be computed by extending the results of Sychra's (1972) equation. The result of the extension is

$$S(\mathbf{R}_0,v)=\int\left[\int_{v=\eta} G^2(\mathbf{R}_0,x,y,z)Z(x,y)\,|\nabla v|^{-1}ds\right]dz, \quad (1)$$

where $\mathbf{R}_0=\mathbf{R}_0(x_0,y_0)$ is the radar sample volume center relative to the vortex center, $ds=[(dx)^2+(dy)^2]^{\frac{1}{2}}$, $Z(x,y)$ is the effective reflectivity factor, and $v(x,y)$ is the velocity normalized to its maximum. The inner integral is performed along the line $s=s(x,y)$ on which $v(x,y)=\eta$, where η is a constant defining a normalized isodop surface. Therefore $S(\mathbf{R}_0,v)$ is the intensity of a spectral component at velocity v and for a specific sample volume position $\mathbf{R}_0$. G^2 is the normalized two-way weighting function of the pulse volume illumination. Integration is recognized as a surface integral with element area $ds\,dz$. Note that both $Z(x,y)$ and ∇v are independent of z; however, G^2 depends on z. Briefly, at each point x,y along this strip, the reflectivity is multiplied with corresponding two-way antenna pattern. The gradient term adjusts the isodops' contribution according to their density (i.e., the closer the isodops are spaced the smaller is the weight applied to the spectral components in the velocity interval between two isodops). To account for contributions of other infinitesimal strips within the sample volume, integration is performed along the third (z axis) dimension. It is assumed that the vortex can be approximated with a combined Rankine model (Lewis and Perkins, 1953) of vortex strength Γ and sink strength $-Q$. All distances are normalized to the radius (assumed equal for radial and tangential velocities) of maximum wind speed so that the velocity profiles are as shown on the upper portion of Fig. 1. The equations describing those profiles are:

$$V_T=\begin{cases} V_{T,\max}r, & \text{for } r\lesssim 1 \\ V_{T,\max}r^{-1}, & \text{for } r\gtrsim 1 \end{cases}$$
$$V_R=\begin{cases} V_{R,\max}r, & \text{for } r\lesssim 1 \\ V_{R,\max}r^{-1}, & \text{for } r\gtrsim 1 \end{cases} \quad (2)$$

where r is a dimensionless radius normalized to the radius of maximum wind.

Consider a Doppler radar viewing the circular flow and assume the radar is at a sufficiently large distance so that the measured Doppler velocity can be approximated by the y component of the velocity vector. It can be shown that this component, normalized to its maximum value, is

$$v=\begin{cases} r\cos(\phi-\alpha), & \text{for } r\lesssim 1 \\ r^{-1}\cos(\phi-\alpha), & \text{for } r\gtrsim 1 \end{cases} \quad (3)$$

where $\alpha=\tan^{-1}Q/\Gamma$ (Fig. 2). The angle ϕ is measured between the y axis and the direction of tangential velocity V_T.

Studies by Ying and Chang (1970) show that the radius of maximal tangential velocity and maximal radial velocity in a laboratory-generated vortex do not coincide, but that the maximal radial velocity radius is larger. Easterbrook and Joss (1973) suggest that this fact and particle drag may create stable circular orbits for particles between the two radii. For this reason we assume that the vortex reflectivity profile peaks near the maximal tangential velocity (Fig. 1b). In the present study we assume coincidence of the maximum tangential and radial velocities with an independent reflectivity profile in order to simplify the simulation. A Gaussian reflectivity profile (Fig. 1b) was chosen for computational convenience:

$$Z(r)=Z_m\exp\left[-\frac{1}{2}\left(\frac{r-r_m}{W_z}\right)^2\right]. \quad (4)$$

In the simulation Z is normalized to its maximum Z_m.

When the radar is far away arc lengths from the beam axis can be approximated with corresponding linear distances in the x,z plane so that the normalized

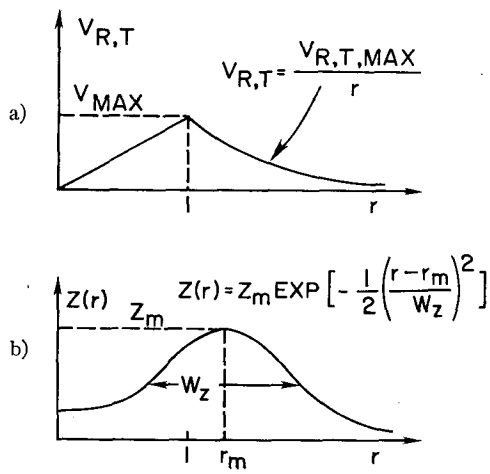

FIG. 1. Profiles of radial and tangential velocity, $V_{R,T}$, and reflectivity, $Z(r)$, for model vortex.

pulse volume illumination is

$$G^2(x_0,y_0,x,y,z)=\frac{\ln 4}{\pi W^2}\exp\left\{-\frac{\ln 4}{W^2}[(x-x_0)^2+z^2]\right\}\times p(y-y_0). \quad (5)$$

Here W is a one-way antenna pattern with half-beamwidth (3 dB) normalized to the vortex radius, and $p(y-y_0)$ is

$$p(y-y_0)=\begin{cases}\dfrac{1}{\Delta R}, & \text{for } |y-y_0|\leq\dfrac{\Delta R}{2}\\ 0, & \text{otherwise}\end{cases} \quad (6)$$

where ΔR is the normalized sample volume depth (Fig. 2).

Fig. 2 shows a cross section in the x,y plane of the vortex isodop velocity field, on which the sample volume and antenna illumination pattern are superimposed. For all simulations the ratio $V_{T,\max}/V_{R,\max}$ is set to 10 ($\tan\alpha=0.1$) and the radius of maximum reflectivity to 1.1.

A numerical program integrates, according to Eq. (1), the isodop field inside the pulse volume. It was found that integration along z had negligible influence on spectrum shape and hence all spectra presented have been calculated from a two-dimensional integration (Fig. 2). The third dimension's effect on relative spectra strengths was accounted for by multiplying the two-dimensional results with $2W$. If we assume the vortex to consist of an infinitely thin rotating shell and no radial inflow, spectrum calculations based on (1) reduce exactly to Lhermitte's (1964) result.

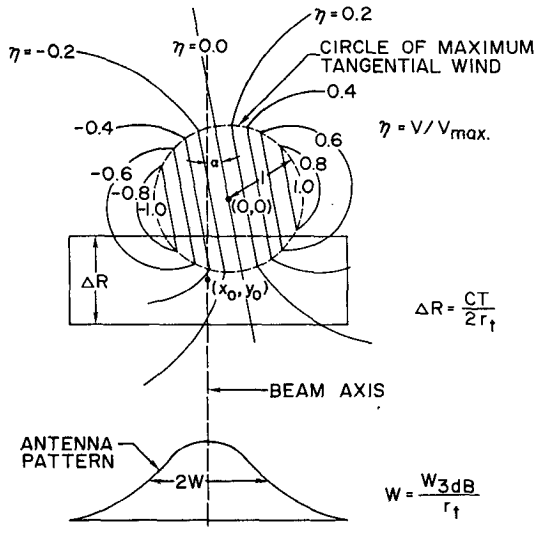

FIG. 2. Horizontal cross section of simulation geometry and antenna pattern. Normalized pulse volume, normalized sample volume depth ΔR, and isodops η are drawn in the horizontal x, y, plane. r_t is the tornado radius.

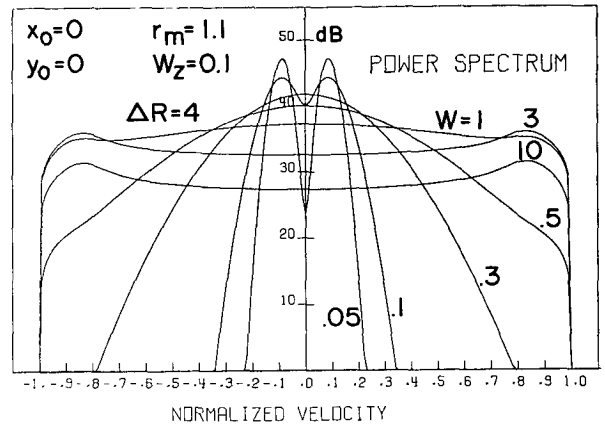

FIG. 3. Simulated vortex spectra. Antenna radar pattern width $2W$ is variable. Sample volume center coincides with the vortex center ($x_0=0$, $y_0=0$) and its depth is four times the size of the vortex radius $\Delta R=4$. The reflectivity profile is as shown in Fig. 1b.

Figs. 3, 4 and 5 represent simulated spectra samples with variable parameters as indicated.

For Fig. 3 the antenna beamwidth $2W$ is varying while the pulse volume is centered on the vortex with $W_z=0.1$ and a tornado diameter one-half the pulse volume depth. For a 1 μs pulse duration the tornado diameter would be 75 m. Both narrow and broad beamwidths may produce bimodal spectra. In the case of narrow beamwidths ($W_z=0.05$), the peaks, very pronounced, are due to the "shell" shaped reflectivity profile combined with the radial inflow. This inflow tilts the isodops at an angle α in the x,y plane (Fig. 2). A centered antenna then can resolve the negative (front side) and positive (back side) velocities. Contributions between those velocities are suppressed by the low reflectivity in the vortex center. Experiments with narrow beamwidth systems, such as lidars, should verify or reject this model. When the antenna beamwidth is broad, bimodal spectra, not as pronounced, are due to high-reflectivity regions containing a longer integration path for higher velocities. Unipeaks appear in between those two cases.

Spectra resulting from simulating an antenna azimuth scan are shown in Fig. 4. The same vortex parameters are used here, but the antenna half-beamwidth is fixed at $W=0.1$. As is seen, the sharpest drop in spectral components occurs at maximum velocities when they are within the pulse volume.

Finally, Fig. 5 shows how reflectivity variation influences spectra shape for centered sample volumes. It is worth noting that uniform reflectivity also may produce bimodal spectra. This happens when the beamwidth is larger than the vortex diameter and the pulse volume is centered on the vortex. These peaks are caused by the scattering volumes located at $r>1$. This is the region where velocity gradient decreases [hence, the scattering volume contribution per velocity interval is increasing as predicted by (1)] and where

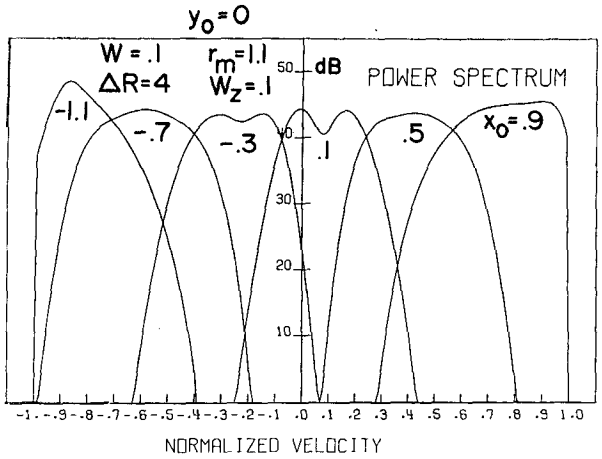

FIG. 4. Simulated vortex spectra, with antenna scanning in azimuth: $y_0=0$, x_0 is variable. Antenna half-beamwidth $W=0.1$.

antenna gain decreases as r increases. For $W>1$ and $\Delta R<1$ (so that the gradient term is constant along s) and $y_0=0$, an approximate equation for the spectrum is

$$S(x_0,v)=S_0\left\{\exp\left[-\frac{\ln 4}{W^2}(v-x_0)^2\right]+\frac{1}{v^2}\exp\left[-\frac{\ln 4}{W^2}\left(\frac{1}{v}-x_0\right)^2\right]\right\}, \quad (7)$$

where S_0 is a normalizing constant. The first term in this equation is a spectral contribution from the region $r<1$ and the second term from $r>1$. It can be shown from (7) that the peak in this Doppler spectrum occurs approximately at

$$v_p\approx\frac{(\ln 4)^{\frac{1}{2}}}{W}, \quad (8)$$

which has been verified by simulation. Results of our simulation show that a 30 dB signal-to-noise ratio will be required in order to observe the spectrum skirts when a wide beam is centered on a vortex having spatially uniform reflectivity (Fig. 5). Satisfaction of this requirement will greatly facilitate the measurements of maximal tangential wind velocities in a tornado. Furthermore we note, when the vortex is contained within the pulse volume, a sharp drop in spectral intensity at the limit of maximal velocities (Fig. 3). It is emphasized that the spectra results reported herein are mean spectral representatives of weather spectra which have statistically distributed power estimates in each velocity resolution cell. In any practical application several spectra will need to be averaged or a least-square's fit will be required in order to deduce spectral shape and infer maximal velocities.

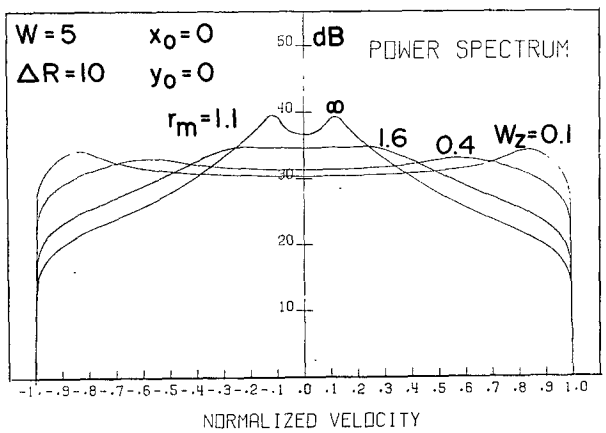

FIG. 5. Simulated vortex spectra with a variable reflectivity profile. Antenna beam is centered ($x_0=0$, $y_0=0$) and the vortex is contained within the pulse volume (depth $\Delta R=10$ and half-beamwidth $W=5$). Reflectivity profile with peak at $r_m=1.1$ has variable width W_z.

3. Observed vortex spectra

In this section a tornado spectrum observed with a cw radar is compared with our simulation. Furthermore, several tornado spectra recorded by an NSSL pulse-Doppler radar are analyzed and compared with simulation results.

In 1961 Smith and Holmes reported a tornado spectrum that was obtained with a cw Doppler radar. Part of their figure is reproduced here as Fig. 6. Since the radar operated in a cw mode, all the detectable motion along the radial is present in the spectra. Positive and negative velocities are superimposed due to the lack of a discriminating circuit. The lower portion of the figure is the superposition of a tornado and parent storm spectra. When the storm spectrum is subtracted, a broad spectrum with a sharp drop at 6 KHz corresponding to 206 mph results. The spectrum in Fig. 6 is similar to those calculated for a large beamwidth ($W>1$) and for vortices having a ring distribution of reflectivity and which are well within the pulse volume [$\Delta R=4$ (Fig. 3)]. Note that the storm spectral components (Fig. 6A) fall slowly into the noise and it appears that the storm may have extremely high velocities. These spectral components may be the higher velocity scatters contributing to the spectrum via the side lobes or they may be caused by the coupling of spectral powers between velocity bins within the spectral analyzer or they may be harmonics. Nevertheless, when the beam is centered on the tornado funnel, the spectrum does exhibit the rapid decrease in intensity as found in the simulation.

Easterbrook and Joss (1973) have recorded spectra of aircraft wing-tip vortices. In their experiments,

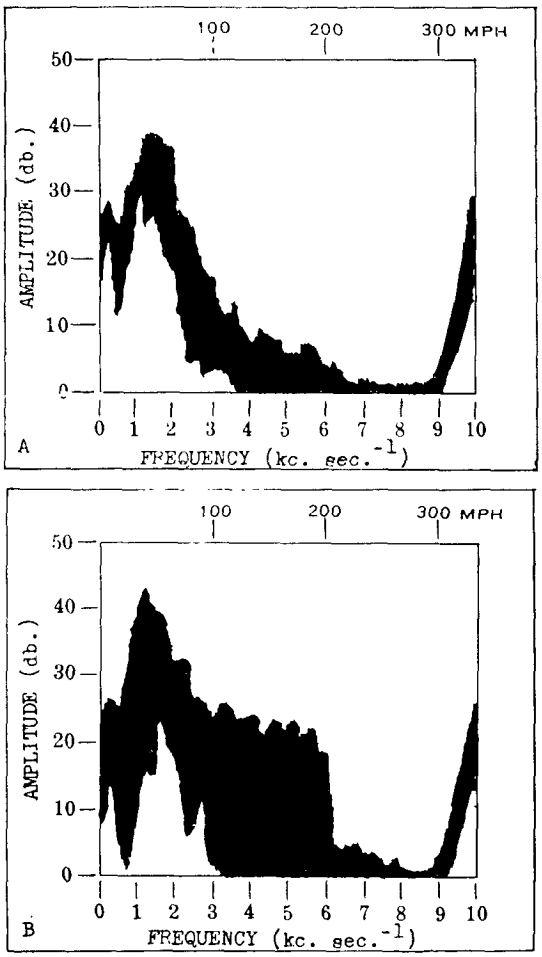

FIG. 6. Doppler spectra observations of Smith and Holmes. Parent storm spectrum is shown in A. High-speed, possibly tornado spectrum signature superimposed is shown in B.

chaff was injected into the vortex that was within the pulse volume. Broad and double peak spectra were noticed and were attributed to a shell-shaped reflectivity profile. This agrees with our double peak spectra obtained from simulation of vortices with similar reflectivity profiles (Fig. 3).

On 23 May 1973 a large tornado formed near Union City in Oklahoma. NSSL's 10 cm high-resolution Doppler radar (0.8° beamwidth, 1 μs pulsewidth) scanned its immediate vicinity while at the same time, laboratory members documented its evolution on film. Digital radar samples were recorded and Fourier-analyzed, and the results of this analysis is presented.

The geometry, antenna beamwidth size, and the visible portion of the vortex are shown in Fig. 7 as a sketch obtained from a photograph. It was found that the reflectivity in the region several square kilometers around the sighted tornado was very high (40–50 dBZ). If the funnel is assumed to have a water content of a cumulus congestus parent cloud, which in favorable conditions can reach 4 g m^{-3}, the reflectivity factor may be at most as high as 13 dBZ and hence the signal contribution from condensation in the funnel should be negligible. The storm's large reflectivity is attributed to sparsely distributed but large rain drops that were noticed by the field scientists located a few kilometers from the tornado. Hence, it is believed that the measured spectra are a result of the large drop trajectories in and around the vortex and/or debris.

Starting at zero elevation, two scan sequences in the immediate tornado vicinity were recorded. Due to the strong return, the I and Q time series components frequently were clipped in the A/D converter. The clippings net effect is the generation of odd harmonics that alternate between positive and negative frequencies (Van Vleck and Middleton, 1966). For broader spectra the effect manifests itself in the rise of noise as the higher, but broader harmonics are folded into the Nyquist co-interval. This was confirmed by comparing clipped and unclipped versions of simulated time series spectra (Zrnic, 1975). It was found that clipping levels 5% above the clipped rms values have only minor effect on the spectral components that lie within 12 dB from the spectral peak. Since the clipping in recorded data was rarely that large, the spectral components up from 12 dB below the peak are considered to be fairly reliable.

Fig. 8 shows an example of a Doppler spectrum for a pulse volume in the vicinity of the Union City tornado. The presence of averaged spectral components (solid line) always above noise level is attributed, in part, to clipping and aliasing of resulting harmonics. The signal spectrum appears to extend from about $+13$ m s^{-1} to the Nyquist limit ($+34.2$ m s^{-1}) and

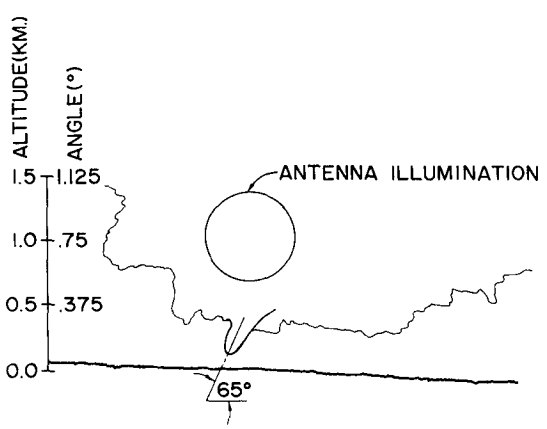

FIG. 7. Beamwidth size (3 dB two-way) and visible vortex size of Union City tornado. Vertical and horizontal scales are identical. Tornado is tilted at about 65°. This sketch is from a photo record at the time when the vortex was just about touching the ground. The first Doppler scan took place within 60 s of the time when this picture was taken.

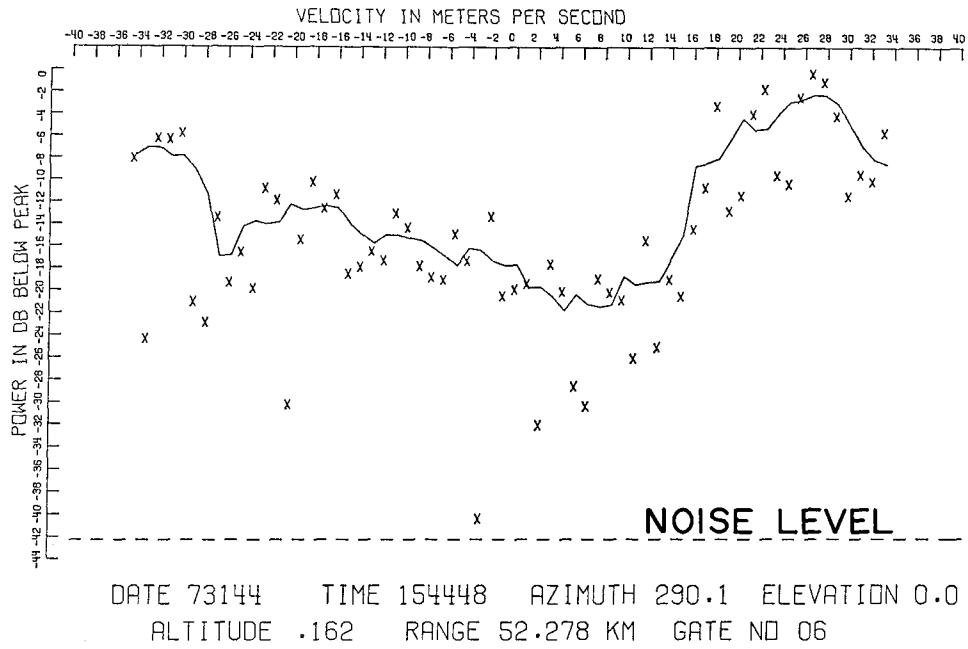

FIG. 8. Spectrum with maximum measured velocity at zero elevation. This spectrum was within 1.5 km of reported tornado touch down. The full line was obtained by averaging five data points for visual clarity. Data points are marked with crosses and the receivers noise level with a dashed line.

continues as an aliased spectrum from -34.2 m s^{-1} to about -26 m s^{-1}. The assignment of an absolute velocity scale requires additional information obtained from comparing Doppler spectra taken at neighboring locations and deducing physically realistic Doppler velocity fields and Doppler shear. Fig. 9a shows a number of sample volume locations with numerical values indicating computed mean Doppler velocities. The spectrum in Fig. 8 is associated with the volume having a 38 m s^{-1} mean. Actually two aliasing corrections are made. We recognize in Fig. 8 that the signal spectrum is aliased and, after deleting all spectral components having magnitudes less than 15 dB below the modal value, we translate by 68.4 m s^{-1} those spectral components divorced from the principal part of the spectrum (i.e., one containing the modal components). The mean Doppler is computed from this reconstructed signal spectrum and 10 m s^{-1} storm motion is added to obtain the 38 m s^{-1} value. The second aliasing correction requires comparison of mean values at neighboring locations. Fig. 9a shows the isodop pattern of mean Doppler fields without this second correction. This pattern is not readily related to any reasonable configuration of wind, whereas Fig. 9b, having mean values corrected (i.e., -68 m s^{-1} added), at two range locations, gives a pattern associated with mesocyclones (Doviak *et al.*, 1974). Thus the maximum velocity in Fig. 8 is actually about -55 m s^{-1} (corresponding to about $+15$ m s^{-1} in the figure). This was the highest velocity that could be reliably deduced from among the hundreds of analyzed Doppler spectra for pulse volumes in the tornado region and does not exclude higher velocities. It is known from the damage on the ground and film data that the maximal tangential wind was faster, but aliasing and strong reflectivity combined with clipping precluded positive identification of those maxima. The visible tornado diameter as measured from photo-

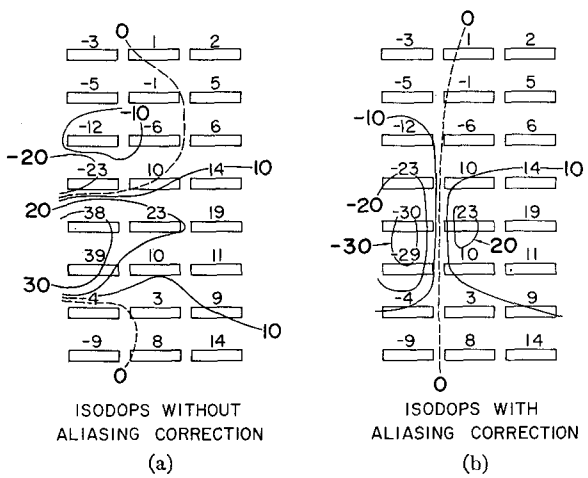

FIG. 9. Mean Doppler velocity fields without and with aliasing correction. The small rectangles (150 m×700 m) represent radar sample volume cross sections through the beam axis. Mean velocities within each pulse volume are in meters per second and are written above the rectangles; 10 m s^{-1} storm motion is subtracted. Gate-to-gate separation in range is 600 m and azimuth 850 m. Aliasing correction is discussed in the text.

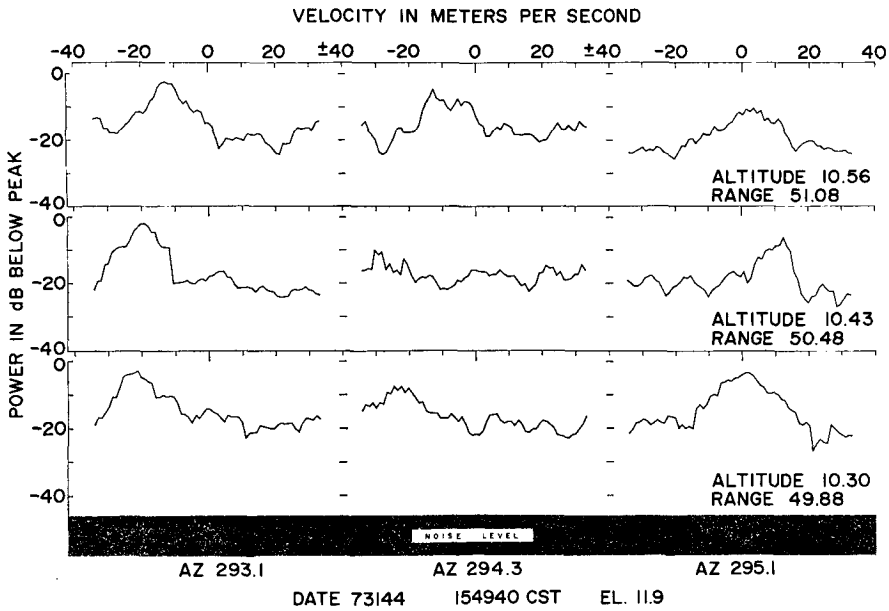

FIG. 10. Spectra at three azimuthal and range locations. Vortex center was very close to the middle gate which has the broadest spectrum. The spectra indicate circular cyclonic flow. The scale is relative to the largest spectral peak. Noise levels are at −45 dB and range and altitude are in kilometers.

graphic film was 200 to 600 m during the time of the Doppler observations reported here.

More spectra at three consecutive azimuthal and range locations taken at an elevation of 11.9° are shown in Fig. 10. The flat spectrum at gate 50.48 km, azimuth 294.3°, is believed to contain contributions from positive and negative velocities beyond the Nyquist limit. Using film documentation and tornado path location in space and time, we determined that the vortex has a position extrapolated to the 10 km height consistent with this gate location. The placement of positive and negative spectral peaks indicate cyclonic motion. The slight shift of the peaks toward negative velocities is attributed to the 8–10 m s^{-1} storm motion toward the radar.

Note the similarity between spectra at range of 50.48 km, at azimuths of 293.1° and 294.3°, with those simulated in Fig. 11 ($x_0 = -2.5$ for azimuth 293.1° and $x_0 = 0$ for azimuth 294.3°). Relative sizes and the geometry were chosen to match the deduced experimental parameters with a reflectivity profile assumed uniform throughout the radar sample volume. Due to the presence of clipping noise, the spectral comparison can only be made with confidence for negative regions of velocity where we have strong spectral components. Their concentration in this region is due to antenna pattern weighting isodops outside the region of maximum tangential velocities. The relatively uniform decrease of spectrum intensity for positive velocities is consistent with the pattern weighting of velocities within the vortex as predicted by simulation (Fig. 11).

Another sequence of spectra taken at a later time and location where the tornado was reported to have touched the ground is shown in Fig. 12. Because two gates (azimuth 295.1° with range +44.48 and 45.08 km) have broad spectra, the tornado center was deduced to be between these gates, a location consistent with ground position. Fig. 13 shows by simulation the change in spectrum width as a function of radial gate position. Reflectivity for these results is

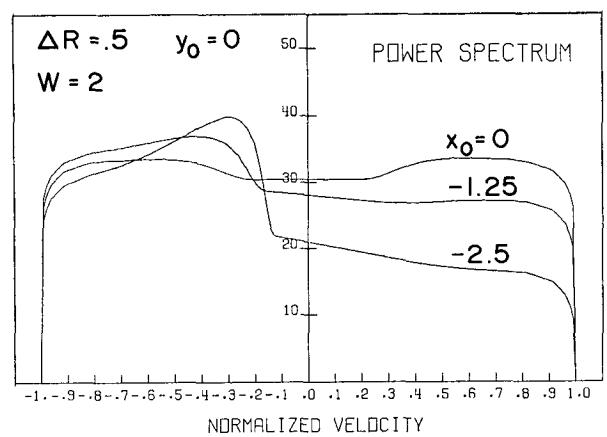

FIG. 11. Simulated spectra of an azimuth scan. The reflectivity is uniform and the dimensions closely match those of the Union City tornado. Tornado diameter model is 600 m. Pulse depth $\Delta R = 0.5$ corresponds to 150 m, and antenna beamwidth $2W = 4$ corresponds to 600 m. At $x_0 = -1.25$ the beam center is offset by −375 m from the tornado axis while at $x = -2.5$ the offset is −750 m.

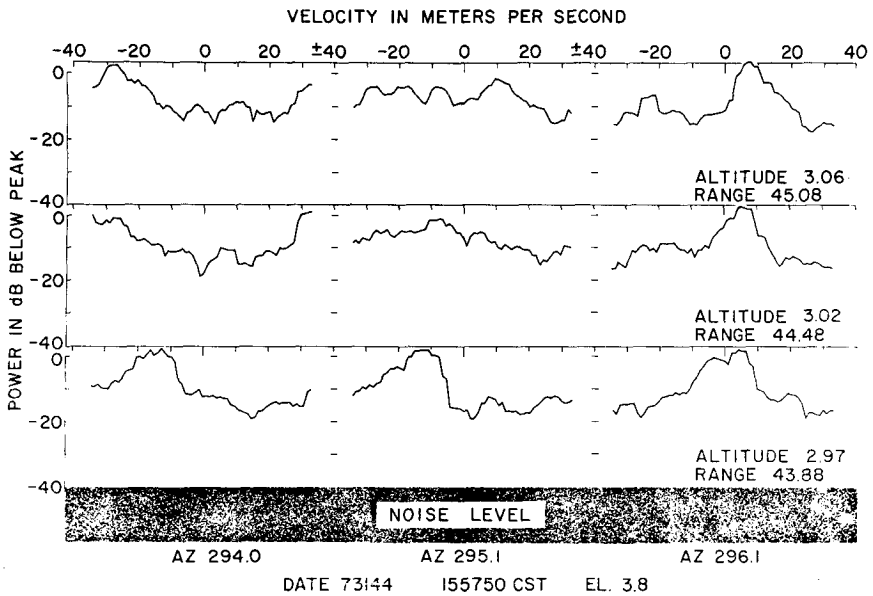

FIG. 12. A sequence of spectra taken at a later location in time and space. Vortex center is between 44.5 and 45 km and at an azimuth of 295.1. Second gate on the left exhibits folding. Noise levels are at −40 dB.

uniform and dimensions match the experiment. The slight asymmetry in spectra position (i.e., a shift toward negative velocities) is due to radial inflow. If the tornado is midway between the two gates having broad spectra (Fig. 12) then the value $y_0 = -1$ would simulate this location. Since the measured spectra probably occupy more than the Nyquist interval, the peak tornado velocity, as deduced from Fig. 13, should be at least $(0.6)^{-1}$ times as large as the Nyquist limit or about 60 m s^{-1}. Folding and sparse gate spacing preclude definite quantitative estimates of tornado parameters, but seemingly at this time the diameter of maximal velocities was close to 600 m.

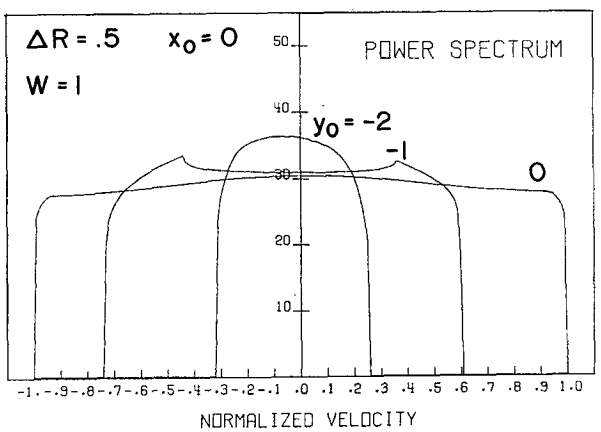

FIG. 13. Simulated spectra resulting from a centered antenna and pulse volume scan in range. Tornado diameter is 600 m. Pulse depth is 150 m, beamwidth 2W corresponds to 600 m, and pulse volume center coincides with the vortex $y_0 = 0$, and is in front of it at −300 m and −600 m.

Cyclonic motion and broad spectra were identified at other elevation angles for both scans. These consistent features coincide with the tornado parameters (position, time, orientation, etc.) as photographed and recorded by the field scientists (Fig. 7).

Because a broad spectrum may be used as an indicator for tornado detection, standard deviations were checked for the various spectra in and around the tornado location. Standard deviations were consistently large where the tornado was present. With NSSL's radar the largest flat spectrum standard deviation that can be measured is $68/(12)^{\frac{1}{2}}$ m s^{-1}, which correspond to all velocity bins being uniformly filled. For illustration, the standard deviations in the 40 gates, including those of Fig. 12, are shown on Fig. 14. As expected the absolute maximum of 17.5 m s^{-1} is found between the gates with broadest spectra. This result is not very dramatic because turbulence within the pulse volume may easily create standard deviations around 3–5 m s^{-1} which is not small compared to the theoretical maximum. It is believed that radars with larger unambiguous velocity intervals should yield more significant maxima in standard deviations when the vortex is within a pulse volume.

4. Conclusion

A computer simulation program is developed to simulate pulse Doppler spectra and to characterize spectral shape as a function of radar and tornado cyclone parameters. When beamwidth is large com-

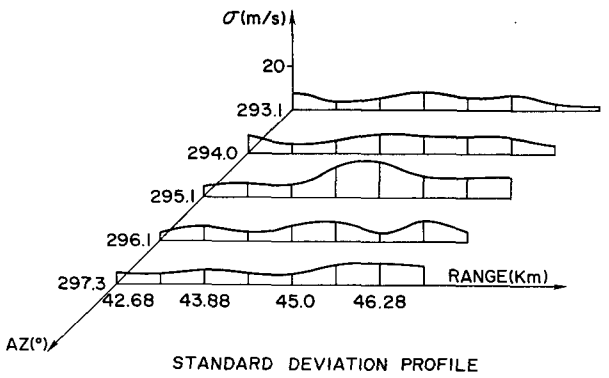

FIG. 14. Standard deviation profile from 40 gates that include those presented on Fig. 12. Measured values at each gate are represented with vertical lines connected along range for visual clarity.

pared to cyclone diameter and reflectivity is concentrated within the region of maximal tangential wind, the spectrum is rather uniform with intensity falling rapidly at the spectrum skirts in agreement with a reported observation. A uniform reflectivity field throughout the cyclone causes a larger proportion of spectral power to be concentrated about zero velocity and simulation shows that a 30 dB signal-to-noise ratio would be required in order to observe spectral skirts.

Pulse-Doppler spectra, observed with the NSSL high-resolution radar, showed clear evidence of tornado cyclone circulation within its pulse volume and qualitative comparison with simulated spectra show agreement. Although the precise vortex center location could not be determined, its position as determined from Doppler spectra observation was consistent with tornado position deduced from film documentation. The simulation predicts bimodal spectra for centered vortices for both uniform and ring reflectivity distributions. Additional experiments, at a higher pulse repetition rate corresponding possibly to unambiguous Doppler velocity of $\pm$ 100 m s^{-1} and with gates covering a continuous region, are needed to reveal the funnel's velocity and reflectivity profile. High-resolution lidar probing, while possibly impractical for tornado detection through severe storms, should offer good hope for the velocity and reflectivity profile determination.

The increased velocity spectrum standard deviation from circulations within the pulse volume can be used as a possible tornado indicator. However, with low PRF and associated folding, the false alarm rate most likely would be excessive.

In the Union City tornado case NSSL's 10 cm Doppler radar measured surprisingly uniform and large reflectivity throughout the cyclone. This was attributed to large drops and debris. When large drops and debris are absent detection of tornadoes with radar at ranges larger than 40 km will be very unlikely due to the small reflectivity of the funnels.

Acknowledgments. We thank Messrs. Holmes and Smith for kindly permitting us the use of their cw Doppler spectrum of a tornado. The pulsed-Doppler tornado spectra have been realized through the dedicated effort of Mr. Dale Sirmans who developed NSSL's Doppler radar and processor into a harmonious system. Messrs. Brown, Burgess and Lemon, through their enduring effort on data reduction and analysis, have helped focus our attention on those data associated with the tornado cyclone. Mr. Bumgarner has provided the necessary computer and programming support and Dr. Golden has led NSSL's field observation team. During part of this work Dr. Zrnic was an NRC postdoctoral fellow at NSSL. Part of this work was supported by the Atomic Energy Commission under Contract AT (49-5)-1289 and the FAA under Contract DOT FA-72-WAI-265.

REFERENCES

Doviak, R. J., D. Burgess, L. Lemon and D. Sirmans, 1974: Doppler velocity and reflectivity structure observed within a tornadic storm. *J. Rech. Atmos.*, **8**, 235–243.

Easterbrook, C. C., and W. W. Joss, 1973: The utility of Doppler radar in the study of aircraft wing tip vortices. Report, Cornell Aeronautical Laboratories, Inc.

Hoecker, W. H., Jr., 1960: Wind speed and air flow patterns in the Dallas tornado of April 2, 1957. *Mon. Wea. Rev.*, **88**, 167–180.

Lewis, W., and P. J. Perkins, 1953: Recorded pressure distribution in the outer portion of a tornado vortex. *Mon. Wea. Rev.*, **81**, 374–385.

Lhermitte, R. M., 1964: Doppler radars as severe storm sensors. *Bull. Amer. Meteor. Soc.*, **45**, 587–596.

Sloss, P. W., and D. Atlas, 1968: Wind shear and reflectivity gradient effects on Doppler radar spectra. *J. Atmos. Sci.*, **25**, 1080–1089.

Smith, R. L., and D. W. Holmes, 1961: Use of Doppler radar in meteorological observations. *Mon. Wea. Rev.*, **89**, 1–7.

Sychra, J., 1972: Relation between real and pulse volume averaged fields of reflectivity and velocity. Canadian Meteorological Service Research Reports.

Van Vleck, J. H., and D. Middleton, 1966: The spectrum of clipped noise. *Proc. IEEE*, **54**, 2–19 (Reprint from 1943 report.)

Ying, S. J., and C. C. Chang, 1970: Exploration model study of tornado-like vortex dynamics. *J. Atmos. Sci.*, **27**, 3–17.

Zrnic, Dusan S., 1975: Simulation of weatherlike Doppler spectra and signals. *J. Appl. Meteor.*, **14**, 619–620.